Journal of Solid State Chemistry 184 (2011) 3095–3103

Contents lists available at SciVerse ScienceDirect

Journal of Solid State Chemistry

journal homepage: www.elsevier.com/locate/jssc

Synthesis and characterization of Pd-poly(N-vinyl-2-pyrrolidone)/KIT-5 nanocomposite as a polymer–inorganic hybrid catalyst for the Suzuki–Miyaura cross-coupling reaction

Roozbeh Javad Kalbasi *, Neda Mosaddegh

Department of Chemistry, Shahreza Branch, Islamic Azad University, 311-86145 Shahreza, Isfahan, Iran

ARTICLE INFO

Article history:
Received 1 May 2011
Received in revised form
24 August 2011
Accepted 14 September 2011
Available online 21 September 2011

Keywords:
Poly(N-vinyl-2-pyrrolidone)
KIT-5
Polymer–inorganic hybrid material
Pd nanoparticles
Suzuki–Miyaura reaction
Aqueous solution

ABSTRACT

Composite poly(N-vinyl-2-pyrrolidone)/KIT-5 (PVP/KIT-5) was prepared by in situ polymerization method and used as a support for palladium nanoparticles obtained through the reduction of $Pd(OAc)_2$ by hydrazine hydrate. The physical and chemical properties of the catalyst were investigated by XRD, FT-IR, UV–vis, TG, BET, SEM, and TEM techniques. The catalytic performance of this novel heterogeneous catalyst was determined for the Suzuki–Miyaura cross-coupling reaction between aryl halides and phenylboronic acid in the presence of water at room temperature. The stability of the nanocomposite catalyst was excellent and could be reused 8 times without much loss of activity in the Suzuki–Miyaura cross-coupling reaction.

1. Introduction

Palladium nanoparticles have become of increasing scientific interest as catalysts for carbon–carbon bond-forming reactions such as Suzuki–Miyaura cross-coupling reactions, which are among the most useful methodologies in advanced organic synthesis [1–4]. The traditional Suzuki–Miyaura reaction generally employs the homogeneous palladium catalysts in the presence of various ligands such as phosphanes, N-heterocyclic carbenes, oxime carbapalladacycle, imidazolium, and Schiffs bases [5–7]. However, the separation and recovery of homogeneous catalysts are not easy, and the resulting products are often contaminated by Pd metal. On the other hand, reusable heterogeneous catalysts are recently attracting much attention due to the increasing international momentum for the development of an environmentally benign reaction in terms of green chemistry [8–10].

In catalytic applications, a uniform dispersion of nanoparticles and an effective control of particle size are usually expected. However, nanoparticles frequently aggregate to yield bulk-like materials, which greatly reduce the catalytic activity and selectivity. Therefore, they must be embedded in a matrix such as polymer or macromolecular organic ligands [11,12]. However, nanoparticle–polymer composites usually suffer from disadvantages such as absence of complete heterogeneity and high temperature annealing, which generally causes thermal degradation of organic polymers. In addition, to avoid the problems associated with metal nanoparticles such as homogeneity, recyclability, and the separation of the catalyst from reaction system, some other works have focused on immobilizing metal nanoparticles on suitable support materials such as immobilization in pores of heterogeneous supports [13,14] like ordered mesoporous silica. Although nanoparticle-mesoporous materials are completely heterogeneous, the hydrophilicity of these catalysts causes a reduction in the activity of such catalysts in organic reactions. Therefore, preparation of organic–inorganic hybrid catalysts with a hydrophobe–hydrophile nature is interesting [15].

Ordered mesoporous silica materials have received considerable attention because of their unique structures with organized porosity, high specific surface area, and specific pore volume, which make them available to a wide range of applications in the areas of adsorption, separation, sensing, and catalysis [16,17]. Among the mesoporous materials, materials that consist of interconnected large-pore cage-type mesoporous systems with three-dimensional (3D) porous networks are highly interesting and promise supports for heterogeneous catalysis. In addition, they are considered to be more advantageous than porous materials that were a hexagonal pore structure with a two-dimensional (2D) array of pores because they allow for a faster

* Corresponding author. Fax: +98 321 3213103.
E-mail address: rkalbasi@iaush.ac.ir (R.J. Kalbasi).

0022-4596/$ - see front matter © 2011 Elsevier Inc. All rights reserved.
doi:10.1016/j.jssc.2011.09.020

diffusion of reactants, avoid pore blockage, provide more adsorption sites, and can be used for processing large-sized molecules [15]. SBA-16, SBA-1, and KIT-5 are a few examples of the porous materials possessing three-dimensional cage-type porous structures [18–20]. Among them, KIT-5, discovered by Ryoo et al., is highly well-ordered cage type mesoporous with cubic *Fm3m* close packed symmetry, high surface area, large pores, and a high specific pore volume [21].

Hybrid organic–inorganic polymers have received increasing interest from research groups because of their unique properties [22–25]. Nevertheless, among the different researches on these materials, there are relatively a few reports on the application of organic–inorganic hybrid polymer as a heterogeneous catalyst [26–29]. Recently, in our previous studies [30–33], hybrid organic–inorganic polymers were used as catalysts.

The hybrid materials could be obtained by combining organic polymers with inorganic materials [34]. These organic–inorganic hybrid materials could be prepared by various methods, depending on what kind of interaction is employed between organic polymers and inorganic elements, or on how organic moieties are introduced to inorganic phases. An in situ polymerization, which is the simultaneous polymerization of organic monomers in the presence of mesoporous materials, is an important method for the preparation of composite materials without chemical interaction.

In continuing our previous works to develop new organic–inorganic hybrid materials as heterogeneous catalysts [30–33], herein, we will introduce a simple and environmentally benign catalyst using a cage-type mesoporous system with three-dimensional (3D) porous networks (KIT-5). The catalytic activity of this novel organic–inorganic hybrid nanocomposite (Pd-poly(N-vinyl-2-pyrrolidone)/KIT-5) was tested for Suzuki–Miyaura cross-coupling reaction. Over this catalyst, Suzuki–Miyaura cross-coupling reaction of aryl halides (X=I, Br, Cl) and phenylboronic acid was successfully carried out in neat water as solvent at room temperature without the use of a ligand such as phosphine derivatives, in reasonable times. This catalyst was easily prepared and can be reused several times (at least 8) without significant loss of activity/selectivity.

2. Experimental method

2.1. Catalyst characterization

The samples were analyzed using FT-IR spectroscopy (using a Perkin Elmer 65 in KBr matrix in the range of 4000–400 cm^{-1}). The BET specific surface areas and BJH pore size distribution of the samples were determined by adsorption–desorption of nitrogen at liquid nitrogen temperature, using a Series BEL SORP 18. The X-ray powder diffraction (XRD) of the catalyst was carried out on a Bruker D8Advance X-ray diffractometer using nickel filtered Cu $K\alpha$ radiation at 40 kV and 20 mA. Moreover, scanning electron microscope (SEM) studies were performed on Philips, XL30, SE detector. The thermal gravimetric analysis (TGA) data were obtained by a Setaram Labsys TG (STA) in a temperature range of 30–650 °C and heating rate of 10 °C/min in N_2 atmosphere. Transmission electron microscope (TEM) observations were performed on a JEOL JEM.2011 electron microscope at an accelerating voltage of 200.00 kV using EX24093JGT detector in order to obtain information on the size of Pd nanoparticles and the DRS UV–vis spectra were recorded with JASCO spectrometer, V-670 from 190 to 2700 nm.

2.2. Catalyst preparation

2.2.1. Preparation of KIT-5

The large pore cage-type mesoporous silica, denoted KIT-5, was prepared using Pluronic F127 ($EO_{106}PO_{70}EO_{106}$) template as a structure directing agent and tetraethylorthosilicate (TEOS) as the silica precursor. In a typical synthesis, 2.5 g (0.198 mmol) of F127 was dissolved in 120 g (6.60 mol) of distilled water and 5.25 g (0.05 mol) of concentrated hydrochloric acid (35 wt% HCl). To this mixture, 12 g (0.057 mol) of TEOS was added. The mixture was stirred at 45 °C for 24 h for the formation of the mesostructured product. Subsequently, the reaction mixture was heated for 24 h at 95 °C under static conditions for hydrothermal treatment. The solid product was then filtered, washed with deionized water and dried at 100 °C. Finally, the samples were calcined at 550 °C for 6 h to remove the template.

2.2.2. Preparation of poly(N-vinyl-2-pyrrolidone)/KIT-5 (PVP/KIT-5)

N-Vinyl-2-pyrrolidone (NVP) (0.5 mL, 4.6 mmol) and KIT-5 (0.5 g) in 7 mL tetrahydrofuran (THF) were placed in a round bottom flask. Benzoyl peroxide (3 mol%, 0.034 g) was added and the mixture was heated to 65–70 °C for 5 h while being stirred under N_2 gas. The resulting white fine powder composite (PVP/KIT-5) was collected by filtration, washed several times with THF, and finally dried at 60 °C under reduced pressure.

2.2.3. Preparation of Pd nanoparticle-poly(N-vinyl-2-pyrrolidone)/KIT-5 (Pd-PVP/KIT-5)

Poly(N-vinyl-2-pyrrolidone)/KIT-5 (PVP/KIT-5) (0.5 g) and 10 mL of an aqueous acidic solution (CHCl=0.09 M) of $Pd(OAc)_2$ (0.053 g, 0.236 mmol) were placed in a round bottom flask. The mixture was heated to 80 °C for 5 h while being stirred under N_2 gas. Then, 0.6 mL (9.89 mmol) aqueous solution of hydrazine hydrates ($N_2H_4 \cdot H_2O$) (80 vol%) was added to the mixture drop by drop in 15–20 min. After that, the solution was stirred at 60 °C for 1 h. Afterwards, the solid was filtered and washed sequentially with chloroform and methanol to remove excess $N_2H_4 \cdot H_2O$ and was dried at room temperature to yield palladium nanoparticle-poly(N-vinyl-2-pyrrolidone)/KIT-5 composite (Pd-PVP/KIT-5) (Scheme 1). The Pd content of the catalyst was estimated by decomposing the known amount of the catalyst by perchloric acid, nitric acid, hydrofluoric acid, hydrochloric acid, and Pd content was estimated by inductively coupled plasma atomic emission spectrometry (ICP-AES). The Pd content of the catalyst estimated by ICP-AES was 0.374 mmol g^{-1} (catalyst Pd loading was 4 wt%).

2.3. General procedure for Suzuki–Miyaura coupling reaction

In the typical procedure for Suzuki–Miyaura coupling reaction, a mixture of iodo benzene (1 mmol), phenylboronic acid (1.5 mmol), K_2CO_3 (5 mmol), and catalyst (0.12 g, Pd-PVP/KIT-5) in H_2O (5 mL)

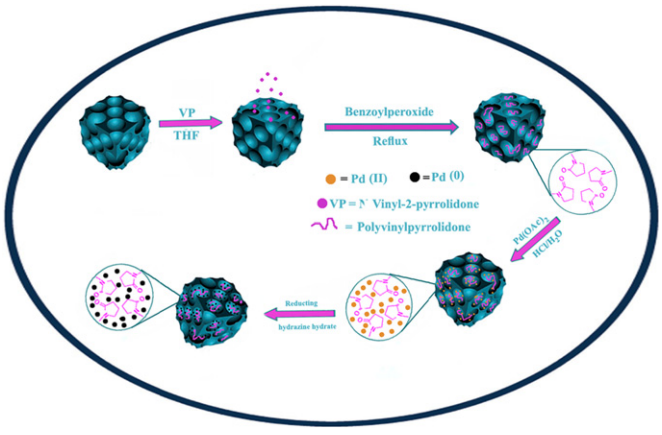

Scheme 1. Encapsulation of PVP and Pd in the 3-D interconnected pore channels of KIT-5.

was placed in a round bottom flask (Pd/iodo benzene molar ratio: 0.0448). The suspension was stirred at room temperature for 5 h. The progress of reaction was monitored by Thin Layer Chromatography (TLC) using n-hexane as eluent. After completion of the reaction (monitored by TLC), for the reaction work-up, the catalyst was removed from the reaction mixture by filtration, and then the reaction product was extracted with CH_2Cl_2 (3×5 mL). The solvent was removed under reduced pressure. The crude product was purified by flash column chromatography (hexane or hexane/ethyl acetate) to afford the desired coupling product (97% isolated yield). The product was identified with ^{1}H NMR, ^{13}C NMR, and FT-IR spectroscopy techniques.

3. Results and discussion

3.1. Catalyst characterization

Fig. 1 shows the powder XRD patterns of the silica KIT-5, PVP/KIT-5 and Pd-PVP/KIT-5. Purely siliceous KIT-5 exhibits three reflections in the region $2\theta = 0.7–3^\circ$, which can be indexed to the (111), (200), and (220) reflections of the cubic space group *Fm3m* [20]. The PVP/KIT-5 and Pd-PVP/KIT-5 ($2\theta = 0.7–10$) samples show the same pattern indicating that the structure of the KIT-5 (100) is well retained even after immobilization with PVP and Pd (Fig. 1). However, the intensity of the characteristic reflection peaks of the PVP/KIT-5 and Pd-PVP/KIT-5 ($2\theta = 0.7–10$) samples are found to be reduced (Fig. 1). This may be attributed to the symmetry destroyed by the hybridization of KIT-5, which is also found in the ordered mesoporous silica loading with guest matter [35]. In addition, composites contain much less KIT-5 due to the dilution of the silicious material by PVP and Pd; therefore, this dilution can also account for a decrease in the peak intensity.

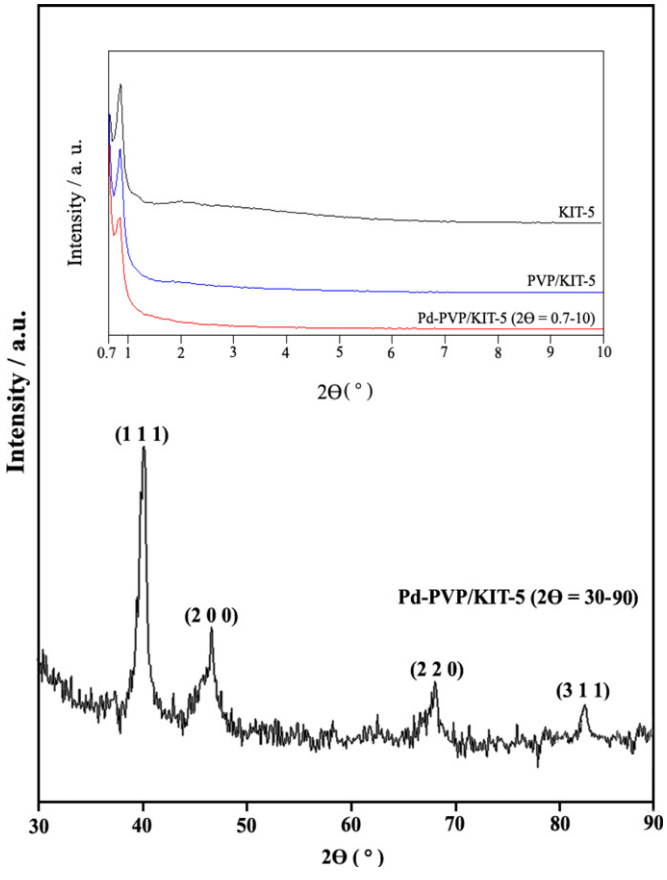

Fig. 1. Powder XRD patterns of (a) mesoporous silica KIT-5, (b) PVP/KIT-5, and (c) Pd-PVP/KIT-5.

The length of the cubic cell a_0 is calculated using the formula $a_0 = d_{111}\sqrt{3}$ (Table 1). The increase in the d-spacing (or the pore center distance a_0) results from the expansion of the pore array structure in Pd-PVP/KIT-5. Compared to the d-spacing (or the pore center distance a_0) of KIT-5 and PVP/KIT-5, the incorporation of the Pd nanoparticles into the PVP/KIT-5 pores leads to the expansion of the KIT-5 pore array (Table 1). These results are in good agreement with that obtained from BET observations.

The wide-angle XRD pattern of the Pd-PVP/KIT-5 nanocomposite ($2\theta = 30–90^\circ$) (Fig. 1) shows the reflections at 39.92°, 46.54°, 67.90°, and 81.84° and these peaks correspond to (111), (200), (220), and (311) lattice planes of Pd nanoparticles [36]. Planes were assigned by comparing them with Pd standard and these planes correspond to the *fcc* crystal lattice structure of Pd (JCPDS, Card No. 05–0681). The crystallite size of Pd particles was evaluated using Scherrer equation for the (220) peak and is found to be approx. 7 nm in size. The size of the Pd nanoparticles, determined using TEM analysis, is more reliable than that determined using Scherrer formula in XRD analysis.

Fig. 2 presents the FT-IR spectra of KIT-5 (a), PVP/KIT-5 (b), and Pd-PVP/KIT-5 (c). Similar to mesoporous silica KIT-5 (Fig. 2a), PVP/KIT-5 and Pd-PVP/KIT-5 samples show the typical vibrations of asymmetric and symmetric stretching as well as the rocking of Si–O–Si at around 1080, 816, and 458 cm^{-1} (Fig. 2). The band at around 950 cm^{-1} is related to Si–OH vibrations of the surface silanols (Fig. 2), which is characteristic of mesoporous silica. The existence of PVP in the PVP/KIT-5 composite is evidenced by the appearance of typical PVP vibration on the FTIR spectrum (Fig. 2b). In the FT-IR spectrum of PVP/KIT-5 (Fig. 2b), the new band at 1663 cm^{-1} corresponds to the carbonyl bond of PVP [37]. Moreover, the presence of peaks at around 2800–3000 cm^{-1} corresponds to the aliphatic C–H stretching in PVP/KIT-5 (Fig. 2b). The appearance of the above bands shows that PVP has been attached to the surface of KIT-5 and the PVP/KIT-5 has been obtained.

As shown in Pd-PVP/KIT-5 spectrum (Fig. 2c), the band around 1663 cm^{-1}, which corresponds to carbonyl bond of PVP, is shifted to lower wave numbers (1639 cm^{-1}) (red shift). Moreover, the peak intensity of the carbonyl bond in the spectrum of Pd-PVP/KIT-5 is lower than that of PVP/KIT-5. This may be due to the interaction between the Pd nanoparticles and C=O groups. This means that the double bond CO stretches become weak by coordinating with Pd nanoparticles. Thus, it is confirmed that PVP molecules exist on the surface of the Pd nanoparticles, and coordinate with the Pd nanoparticles [37–39].

The BET specific surface areas and the pore size of the host KIT-5, PVP/KIT-5, and Pd-PVP/KIT-5 were calculated using Brunauer–Emmett–Teller (BET) and Barrett–Joyner–Halenda (BJH) methods, respectively (Table 1). All the samples exhibit a type IV adsorption

Table 1
Physicochemical properties of mesoporous silica KIT-5, PVP/KIT-5, and Pd-PVP/KIT-5 samples obtained from XRD and N_2 adsorption.

Sample	BET surface area ($m^2\ g^{-1}$)	V_P ($cm^3\ g^{-1}$) [a]	BJH pore diameter (nm)	d_{111} (nm)	a_0 (nm) [b]
Mesoporous silica KIT-5	1090	0.71	2.62	10.38	17.98
PVP/KIT-5	611	0.41	2.68	10.51	18.20
Pd-PVP/KIT-5	305	0.40	5.48	11.13	19.27

[a] Total pore volume.
[b] Unit cell parameter.

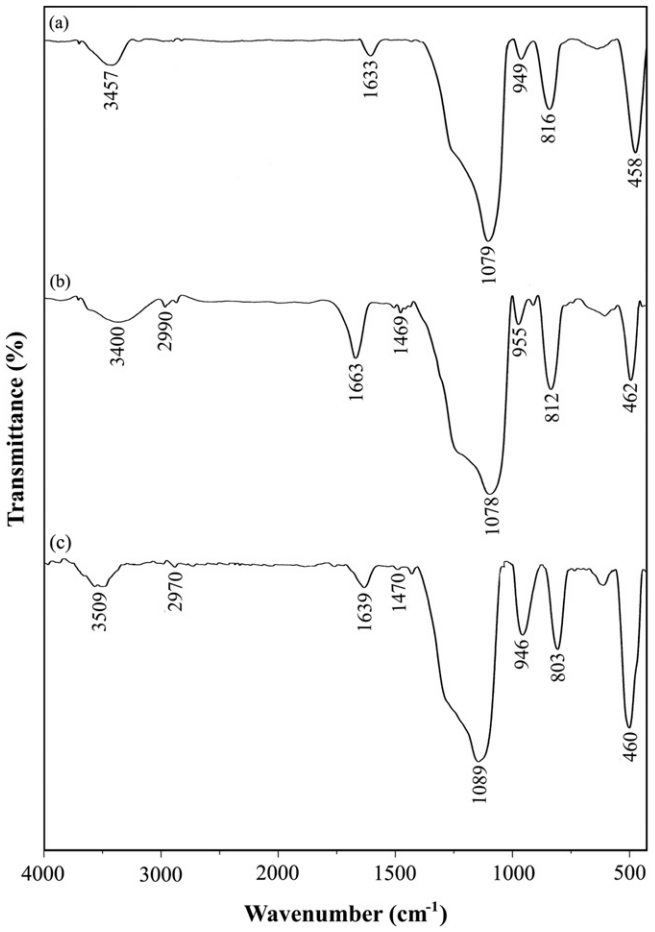

Fig. 2. FT-IR spectra of (a) mesoporous silica KIT-5, (b) PVP/KIT-5, and (c) Pd-PVP/KIT-5.

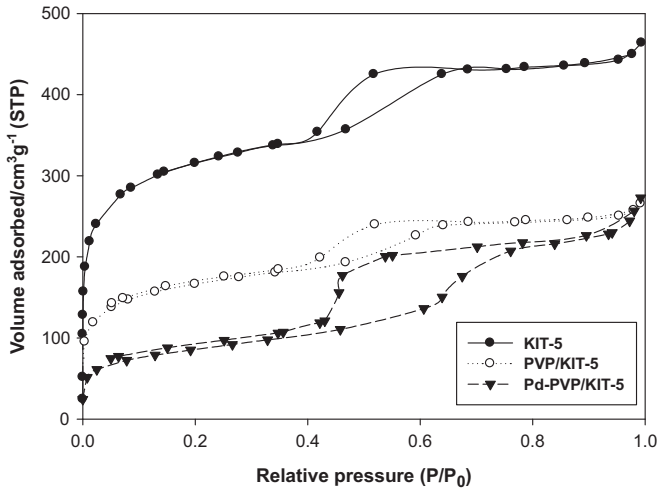

Fig. 3. N_2 adsorption–desorption isotherms of mesoporous silica KIT-5, PVP/KIT-5, and Pd-PVP/KIT-5.

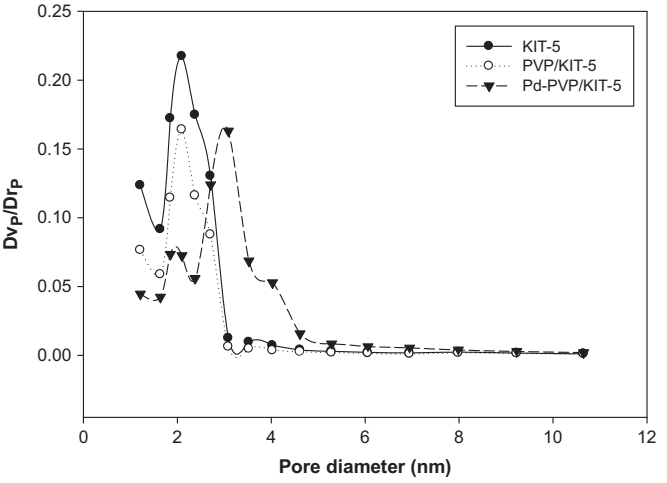

Fig. 4. Pore diameter distributions of KIT-5, PVP/KIT-5, and Pd-PVP/KIT-5.

isotherm with an H2 hysteresis loop, which is typically observed for the mesoporous samples with a cage-type pore structure (Fig. 3). The corresponding BJH pore size distribution curves for the KIT-5, PVP/KIT-5, and Pd-PVP/KIT-5 materials are shown in Fig. 4. It is known that calcined KIT-5 has a high BET surface area (1090 $m^2\,g^{-1}$), a large pore volume (0.71 $cm^3\,g^{-1}$) and pore size (2.62 nm), indicative of its potential application as a host in organic materials. It is clear that PVP/KIT-5 and Pd-PVP/KIT-5 exhibit a smaller specific surface area in comparison to those of pure KIT-5 (611 and 305 $m^2\,g^{-1}$, respectively) (Table 1).

As we can see in Table 1, BJH pore diameter of PVP/KIT-5 after polymerization of PVP on the surface of KIT-5 did not show any significant changes (there is some increase in BJH pore diameter). But we cannot conclude that the polymer chains were not entered in the pores. As we can see in Table 1, the pore volume of PVP/KIT-5 (0.41 cm^3/g) is lower than that of KIT-5 (0.71 cm^3/g). So, we can say that polymerization of NVP has occurred in the channels of KIT-5. This polymerization can cause to produce some pressure on the KIT-5 structure (physical pressure on the wall of the channels) and it can increase the pore diameter (2.68 nm). Moreover, if we notice on the amount of d-spacing, we can see some increase in the amount of d_{111}, which confirms our hypothesis.

In addition, there is a noticeable increase in pore diameter for Pd-PVP/KIT-5, and the pore volume of Pd-PVP/KIT-5 is a little smaller than that of PVP/KIT-5. It might be due to the incorporation of Pd nanoparticles into PVP/KIT-5. Similar results were reported for Pt encapsulated in SBA-15 [40,41].

Although there is significant decrease in the surface area, Pd-PVP/KIT-5 pores were not blocked by deposition of polymers and Pd nanoparticles (Table 1). Hence, Pd-PVP/KIT-5 still has a mesoporous form with a reasonable surface area (305 $m^2\,g^{-1}$) and it is suitable to act as a catalyst.

Fig. 5 presents the TGA curves of KIT-5 (a), PVP (b), PVP/KIT-5 (c), and Pd-PVP/KIT-5 (d) under N_2 atmosphere. The mass loss at temperature $<100\,^{\circ}C$ (around 3.5%, w/w) is attributed to desorption of water present in surfaces of the KIT-5 (Fig. 5a). The TGA curve of PVP shows a small mass loss (around 7.5%, w/w) in the temperature range 50–150 °C, which is apparently associated with adsorbed water (Fig. 5b). At temperatures above 200 °C, PVP shows one main stage of degradation. The mass loss for PVP in the second step is equal to 77% (w/w), which corresponds to the effective degradation of the polymer (Fig. 5b). Thermo analysis of PVP/KIT-5 shows two steps of mass loss (Fig. 5c). The first step (around 3%, w/w) that occurs at 70 °C is related to desorption of water. The second step (around 9%, w/w), which appeared at 270 °C is attributed to degradation of the polymer, and the degradation ended at 580 °C (Fig. 5c). By comparing the PVP and PVP/KIT-5 curves, one can find that the weight loss of PVP/KIT-5 occurs at a higher temperature, which shows that PVP/KIT-5 has higher thermal stability and slower degradation rate than PVP (Fig. 5b and c). However, for Pd-PVP/KIT-5 sample, two separate weight loss steps are seen (Fig. 5d). The first step (around 2%, w/w) appearing at temperature $<100\,^{\circ}C$ corresponds

to the loss of water. The second weight loss (about 500–580 °C) amounts around 4% (w/w) is related to the degradation of the polymer. Obviously, the hybrid Pd-PVP/KIT-5 shows higher thermal stability than PVP/KIT-5. It may be attributed to the presence of Pd nanoparticles in the composite structure.

The morphologies of the KIT-5 host, PVP/KIT-5, and Pd-PVP/KIT-5 are shown in Fig. 6. KIT-5 host (Fig. 6a), PVP/KIT-5 (Fig. 6b), and Pd-PVP/KIT-5 (Fig. 6c) are agglomerations of small irregular particles. As we can see, there is negligible difference in particle surface morphology between the KIT-5 host, the PVP/KIT-5 composite, and Pd-PVP/KIT-5 nanocomposite, which indicates that the polymerization takes place more in the channels and less on the outer surfaces of the catalyst.

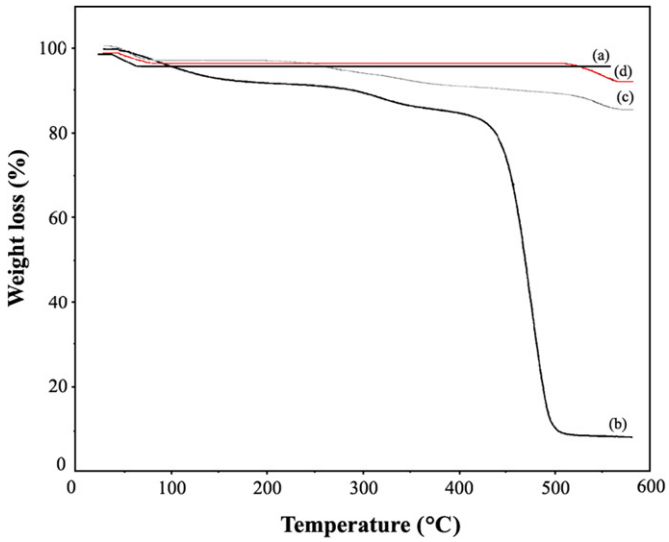

Fig. 5. TGA curves of (a) mesoporous silica KIT-5, (b) PVP, (c) PVP/KIT-5, and (d) Pd-PVP/KIT-5.

Fig. 7 displays the result of UV–vis spectra of Pd-PVP/KIT-5. The UV–vis spectra of $Pd(OAc)_2$, which reveal a peak at 400 nm refer to the existence of Pd(II) [42]. As mentioned in Section 2, and shown in Scheme 1, Pd nanoparticles-PVP/KIT-5 was prepared by adding hydrazine hydrate to the Pd (II)–PVP/KIT-5. However, as can be seen in Fig. 7, there is no peak at 400 nm in the UV–vis spectra of Pd-PVP/KIT-5, which indicates complete reduction of Pd(II) to Pd nanoparticles.

The TEM micrographs of Pd-PVP/KIT-5 are depicted in Fig. 8. Although the image is smeared and dark after the encapsulation of PVP chains and Pd nanoparticles inside the mesochannels (Fig. 8a), the ordered cubic *Fm3m* mesostructure of KIT-5 is retained and no damage in the periodic structure of the silicate framework is observed. The places with darker contrast could be assigned to the presence of Pd particles with different dispersion. This assumption is confirmed by EDX data, where the estimated Pd/Si ratio is about 0.04 and where it correlates with the loaded Pd amount. The small dark spots in the images could be ascribed to Pd nanoparticles, probably located into the support channels.

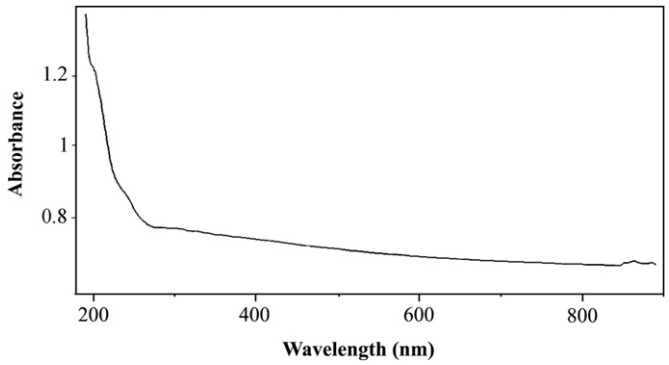

Fig. 7. UV–vis spectra of Pd-PVP/KIT-5.

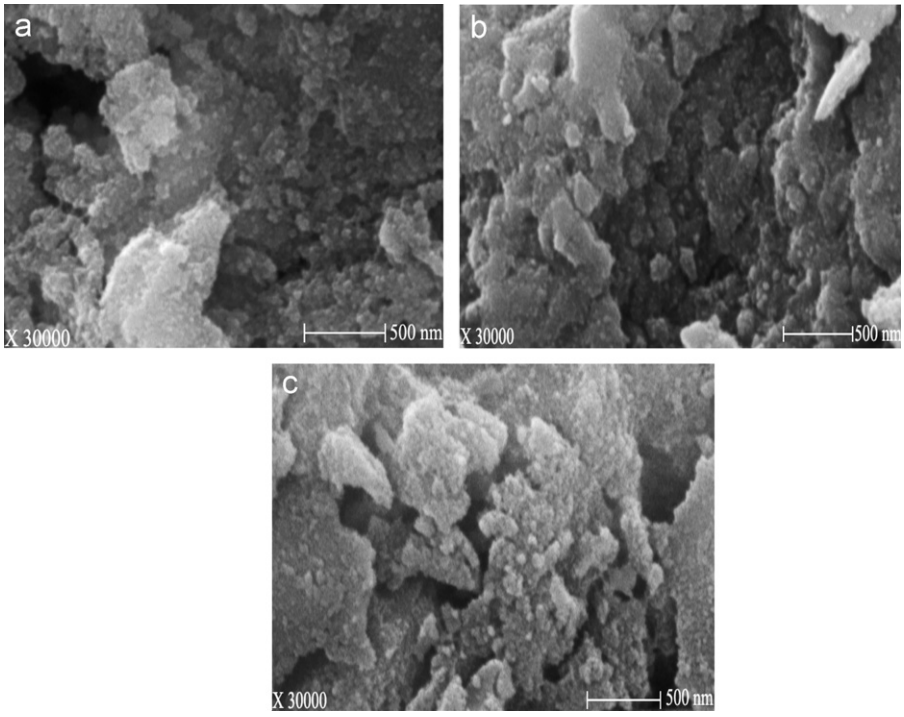

Fig. 6. Scanning electron microscopy (SEM) photographs of (a) mesoporous silica KIT-5, (b) PVP/KIT-5, and (c) Pd-PVP/KIT-5.

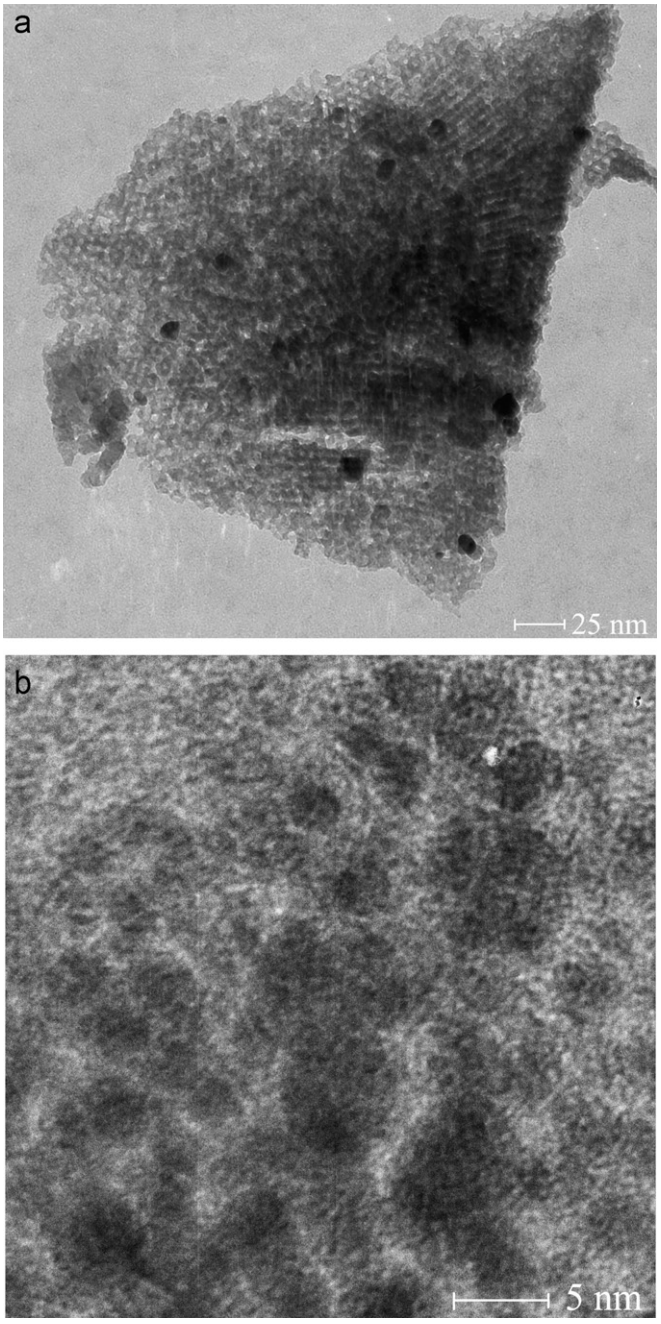

Fig. 8. TEM images for Pd-PVP/KIT-5.

The larger dark areas over the channels most likely correspond to Pd nanoparticle agglomerate on the external surface.

It can be seen from Fig. 8b that spherically shaped palladium nanoparticles (average diameter of ~3–5 nm) were formed (Fig. 8b). It can also be seen that the sizes of Pd nanoparticles are around 3–5 nm, which are a little larger than the silica mesopore diameter (2.6 nm). Similar results were reported for some metal particles encapsulated in the mesoporous structures [43,44]. With the incorporation of the nanoparticles larger than the structure directing agent, pore size can expand the entire mesopore structure uniformly [43,44]. These are in accordance with BET and XRD results. It can be observed in Table 1 that the amount of BJH pore diameter for Pd-PVP/KIT-5 sample (5.48 nm) is higher than the particle size of Pd (3–5 nm). In addition, we can see some small aggregation of Pd nanoparticles in the channels of KIT-5 (Fig. 8b). Therefore, it can be concluded that the aggregation of the nanoparticles increases the pore size up to 5.48 nm.

3.2. Catalytic activity

Pd-PVP/KIT-5 nanocomposite was used as a catalyst for the Suzuki–Miyaura coupling reactions of various aryl halides with phenylboronic acid at room temperature.

To optimize the reaction conditions, a model reaction was carried out by taking iodo benzene and phenylboronic acid in different solvents and bases at room temperature. Solvent plays a crucial role in the rate and the product distribution of Suzuki–Miyaura coupling reactions. Since water is known to increase the activity of the Suzuki–Miyaura catalyst [45,46], two kinds of solvents were used: H_2O or MeOH/H_2O (3:1 v/v), and the reaction was catalyzed with 0.12 g of Pd-PVP/KIT-5 catalyst in the presence of 5 equivalents of base and with an iodo benzene/phenylboronic acid ratio of 1–1.5 (Pd/iodo benzene molar ratio: 0.0448). In recent years, a large number of studies have been devoted by academic and industrial research groups to the development of environmentally benign processes. In this context, the use of water as a reaction medium in transition metal-catalyzed processes has merited increasing attention and is currently one of the most important targets of sustainable chemistry [47]. Water, an inexpensive, readily available, non-inflammable, non-toxic solvent, provides remarkable advantages over common organic solvents both from an economic and an environmental points of view [48,49]. The experimental results show that the time the reaction is completed is shorter in the case of using MeOH/H_2O (3:1 v/v) as a solvent, but neat H_2O was chosen because of the advantages of using water that were mentioned above.

The effect of base on the coupling reaction was evaluated by taking iodo benzene (1 mmol) with phenylboronic acid (1.5 mmol) in water at room temperature in the presence of Pd-PVP/KIT-5 (0.12 g) with various bases (5 mmol) (Pd/iodo benzene molar ratio: 0.0448). The results revealed that the inorganic bases used were more effective than Et_3N (Table 2), and hence, the economically cheaper K_2CO_3 was chosen as base for the coupling reactions.

In order to discriminate the effect of the composite catalyst (Pd-PVP/KIT-5), the reaction occurred over palladium nanoparticles in the same reaction conditions and in this condition, no activity was seen.

Suzuki–Miyaura reactions of different aryl halides and phenylboronic acid with 0.12 g of Pd-PVP/KIT-5 (Pd/aryl halide molar ratio: 0.0448) as catalyst were investigated (Table 3). Reactions were carried out in water at room temperature at different times.

According to the results presented in Table 3, aryl iodides (entries 1, 2, 3, and 6) afforded excellent coupling products in reasonable times. But, among aryl iodides, the coupling of 2-iodo-5-nitrotoluene with phenylboronic acid resulted in moderate yields (60%) at room temperature and the yield did not improve at elevated temperature. It may be due to steric effect of 2-iodo-5-nitrotoluene.

It is well known that activation of C–Cl bond is much more difficult than C–Br and C–I bonds, and in general requires harsher

Table 2
Effect of different bases on Suzuki–Miyaura reaction.[a]

Base	Yield (%) [b]
K_2CO_3	97
Na_3PO_4	70
Et_3N	30

[a] Reaction conditions: Pd-PVP/KIT-5 (0.12 g), iodo benzene (1 mmol), phenylboronic acid (1.5 mmol), base (5 eq), H_2O (5 mL), room temperature, 5 h, Pd/iodo benzene molar ratio: 0.0448.
[b] Isolated yield.

Table 3
Suzuki–Miyaura reaction of aromatic aryl halides and phenylboronic acid catalyzed by Pd-PVP/KIT-5.[a]

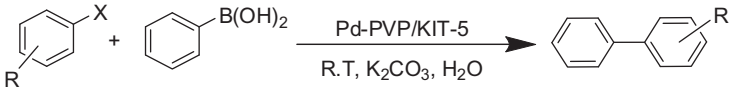

Entry	Substrate	Product	Yield (%) [b]	Time (h)	TOF (h^{-1}) [e]	M_p (°C)	
						Found	Reported [Ref.]
1		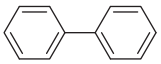	97	5[c]	4.33	71–73	70–72 [67]
2	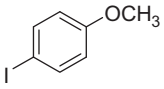	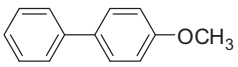	91	7[c]	2.9	92–94	91–92 [67]
3	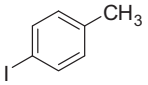	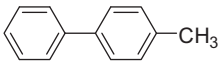	93	2[d]	10.38	47–49	45–50 [67]
4	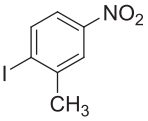	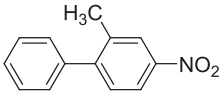	60	12[c]	1.11	53–55	55–56 [68]
5	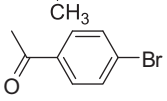	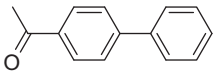	98	1[d]	21.87	121–123	120–122 [67]
6	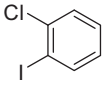	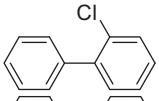	95	2[c]	10.6	31–35	32.5–33.5 [67]
7	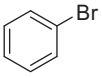	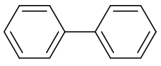	97	9[c]	2.4	71–73	70–72 [67]
8		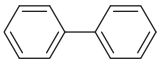	96	12[d]	1.78	71–73	70–72 [67]

[a] Reaction conditions: Pd-PVP/KIT-5 (0.12 g), aryl halide (1 mmol), phenylboronic acid (1.5 mmol), K_2CO_3 (5 eq), H_2O (5 mL), Pd/aryl halide molar ratio: 0.0448.
[b] Isolated yield.
[c] R.T.
[d] 40 °C.
[e] Turn-over frequency.

reaction conditions in heterogeneous catalysis system [50–53]. However, chloro benzene afforded excellent coupling products over Pd-PVP/KIT-5 as catalyst at 40 °C (entry 8), but needed more time than that of aryl iodide.

Thus, the catalyst afforded average to excellent yields of the biaryl products. In the literature, only a few catalysts are known for affecting the Suzuki–Miyaura cross-coupling reactions under mild conditions [54–66].

The turn-over frequency (TOF) value indicates that Pd-PVP/KIT-5 is a good catalyst for this kind of reaction. TOF being defined as the mol product/(mol catalyst. hour); and this was calculated from the isolated yield, the amount of palladium used and the reaction time.

Reusability of the catalyst was tested by carrying out repeated runs of the reaction on the same batch of the catalyst in the case of the model reaction (Table 4). After each cycle, the catalyst was filtered off, washed with water (10 mL), diethyl ether and acetone (3×5 mL). Then, it was dried in oven at 60 °C and reused in the Suzuki–Miyaura reaction. The results show that this catalyst can be reused without any modification, 8 times and no significant loss of activity/selectivity performance was observed. It should be mentioned that there was very low Pd leaching during the reaction and the catalyst exhibits a high stability even after 8 recycles (Table 4). Compared to our previous work on composites prepared, using SBA-15 [30–33], Pd-PVP/KIT-5 shows more recyclability. It can be related to the interconnected large-pore cage-type mesoporous KIT-5 with three-dimensional (3D) porous networks in comparison to SBA-15 with a two-dimensional (2D) array of pores because three-dimensional porous network of KIT-5 allows for a faster diffusion of reactants, avoids pore blockage, provides more adsorption sites and can prevent leaching of PVP and Pd nanoparticles. The amount of Pd leached was determined by ICP-AES technique (Table 4).

Table 4
Catalyst reusability for the Suzuki–Miyaura reaction.[a]

Cycle	Yield (%) [b]	Pd content of catalyst (mmol in 0.12 g catalyst)	Pd leaching (ppm)
Fresh	97	0.0448	–
1	97	0.0448	–
2	96	0.0448	–
3	96	0.0448	–
4	96	0.0448	–
5	95	0.0447	2.1
6	94	0.0447	2.1
7	94	0.0447	2.1
8	93	0.0446	4.2

[a] Reaction conditions: Pd-PVP/KIT-5 (0.12 g), iodo benzene (1 mmol), phenylboronic acid (1.5 mmol), K_2CO_3 (5 eq), H_2O (5 mL), room temperature, 5 h.
[b] Isolated yield.

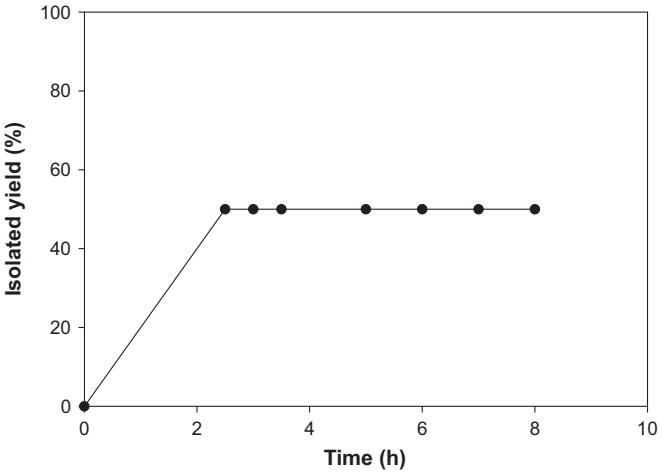

Fig. 9. Heterogeneity test for Suzuki coupling reaction [Reaction conditions: Pd-PVP/KIT-5 (0.12 g), iodo benzene (1 mmol), phenylboronic acid (1.5 mmol), K_2CO_3 (5 eq), H_2O (5 mL), Pd/aryl halide molar ratio: 0.0448].

The XRD patterns of the used catalyst show that the structure of the catalyst maintains. The Pd content of the used catalyst (after 8 cycles) determined by ICP-AES is 0.372 mmol g^{-1} (0.0446 mmol in 0.12 g catalyst) which is about 0.5% lower than the fresh catalyst (Table 4).

In order to prove the heterogeneous nature of the catalyst and the absence of Pd leaching, a heterogeneity test was performed, in which the catalyst was separated from the reaction mixture at approximately 50% conversion of the starting material through centrifugation. The reaction progress in the filtrate was monitored (Fig. 9). No further coupling reaction occurred even at extended times, indicating that the nature of reaction process is heterogeneous and there is not any progress for the reaction in homogeneous phase.

The catalytic activity of Pd-PVP/KIT-5 in Suzuki–Miyaura cross-coupling reaction was compared with Pd/KIT-5 (Pd/KIT-5 was prepared with the same amount of Pd, without using PVP) to investigate the effect of PVP on the activity and stability of the catalyst. The yield of the reaction between iodo benzene and phenylboronic acid over Pd/KIT-5 as catalyst, in water at room temperature, was 76% after 14 h. So, it can be seen that Pd-PVP/KIT-5 shows higher activity in Suzuki–Miyaura cross-coupling reaction at shorter time. Since, the Pd content of Pd-PVP/KIT-5 (0.374 mmol g^{-1}) is almost similar to the Pd/KIT-5 (0.368 mmol g^{-1}), so, it can be related to the hydrophobic nature of Pd-PVP/KIT-5 compared to Pd/KIT-5. It should be mentioned that Pd-PVP/KIT-5 is completely hydrophobe and Pd/KIT-5 is completely hydrophile. Therefore, the organic reactants have a higher tendency to be adsorbed on the surface of Pd-PVP/KIT-5 and consequently the yield will be higher in the case of using Pd-PVP/KIT-5 as catalyst. In addition, interaction of Pd nanoparticles with PVP in Pd-PVP/KIT-5 nanocomposite, prevent the aggregation of Pd nanoparticles in the channels of KIT-5. Therefore, in this condition, more Pd surfaces are available to catalyze the Suzuki–Miyaura cross-coupling reaction and the activity of Pd-PVP/KIT-5 will be higher than Pd/KIT-5.

Furthermore, the reusability of Pd-PVP/KIT-5 in Suzuki–Miyaura cross-coupling reaction was compared with Pd/KIT-5, to investigate the effect of PVP on the stability of the catalyst. The results showed that Pd/KIT-5 could be reused without any modification, 5 times and 13% loss of activity was observed. It should be mentioned that there was 4% Pd leaching during the reaction and the catalyst. Compared to Pd-PVP/KIT-5, Pd/KIT-5 shows less recyclability. It can be related to the interaction of Pd nanoparticles with PVP, which it can prevent leaching of Pd nanoparticles. So, Pd-PVP/KIT-5 showed higher stability than Pd/KIT-5 due to the effect of PVP.

4. Conclusion

A novel polymer–inorganic hybrid material, Pd nanoparticles—PVP/KIT-5, was prepared by a simple method. The catalytic activity of this novel organic–inorganic hybrid was excellent for Suzuki–Miyaura cross-coupling reaction of aryl chloride, bromide, and iodides at room temperature or 40 °C under aerobic conditions. Most importantly, water has been chosen as a green solvent for this reaction. This new heterogeneous catalyst showed following advantages: (a) high catalytic activity under mild reaction conditions; (b) easy separation after reaction; and (c) reusability for several times without any loss in the yield of the reaction. Finally, we believe that the new synthetic method reported here would greatly contribute to an environmentally benign process.

Acknowledgments

The support by the Islamic Azad University, Shahreza Branch (IAUSH) Research Council and Center of Excellence in Chemistry is gratefully acknowledged.

References

[1] R. Narayanan, M.A. El-Sayed, J. Am. Chem. Soc. 125 (2003) 8340–8347.
[2] M. Bernechea, E. de Jesus, C. Lopez-Mardomingo, P. Terreros, Inorg. Chem. 48 (2009) 4491–4496.
[3] T.M. Razler, Y. Hsiao, F. Qian, R. Fu, R. Kashif Khan, W. Doubleday, J. Org. Chem. 74 (2009) 1381–1384.
[4] R. Narayanan, M.A. El-Sayed, J. Phys. Chem. B 108 (2004) 8572–8580.
[5] L. Tao, Y. Xie, C. Deng, J. Li, Chin. J. Chem. 27 (2009) 1365–1373.
[6] X. Chanjuan, W. Yongwei, Y. Xiaoyu, J. Organomet. Chem. 693 (2008) 3842–3846.
[7] S. Koji, T. Ryouta, N. Tsukasa, F. Hisashi, Angew. Chem. Int. Ed. 47 (2008) 6917–6919.
[8] A. Gniewek, J.J. Ziolkowski, A.M. Trzeciaka, M. Zawadzki, H. Grabowska, J. Wrzyszcz, J. Catal. 254 (2008) 121–130.
[9] N.J.S. Costa, P.K. Kiyohara, A.L. Monteiro, Y. Coppel, K. Philippot, L.M. Rossi, J. Catal. 276 (2010) 382–389.
[10] A. Molnar, Chem. Rev. 111 (2011) 2251–2320.
[11] R.A. Sanchez-Delgado, N. Machalaba, N. Ng-a-Qui, Catal. Commun. 8 (2007) 2115–2118.
[12] Y. Luo, X. Sun, Mater. Lett. 61 (2007) 2015–2017.
[13] J.M. Thomas, B.F.G. Johnson, R. Raja, G. Sankar, P.A. Midgley, Acc. Chem. Res. 36 (2003) 20–30.
[14] M. Jacquin, D.J. Jones, J. Roziere, Appl. Catal. A: Gen. 251 (2003) 131–141.
[15] S. MacQuarrie, B. Nohair, J.H. Horton, S. Kaliaguine, C.M. Crudden, J. Phys. Chem. C 114 (2010) 57–64.
[16] B.J. Scott, G. Wirnsberger, G.D. Stucky, Chem. Mater. 13 (2001) 3140–3150.
[17] A. Taguchi, F. Schuth, Micropor. Mesopor. Mater. 77 (2005) 1–45.
[18] E.M. Rivera-Muñoz, R. Huirache-Acuña, Int. J. Mol. Sci. 11 (2010) 3069–3086.
[19] M.-C. Liu, C.-S. Chang, J.C.C. Chan, H.-S. Sheu, S. Cheng, Micropor. Mesopor. Mater. 121 (2009) 41–51.
[20] W. Cheng-Yu, H. Ya-Ting, Y. Chia-Min, Micropor. Mesopor. Mater. 117 (2009) 249–256.
[21] F. Kleitz, D. Liu, G.M. Anilkumar, I.-S. Park, L.A. Solovyov, A.N. Shmakov, R. Ryoo, J. Phys. Chem. B 107 (2003) 14296–14300.
[22] J.E. Mark, Acc. Chem. Res. 39 (2006) 881–888.
[23] J. Zheng, G. Li, X. Ma, Y. Wang, G. Wu, Y. Cheng, Sens. Actuators B 133 (2008) 374–380.
[24] C.M. Chung, S.J. Lee, J.G. Kim, D.O. Jang, J. Non-Cryst. Solids 311 (2002) 195–198.
[25] N. Ostapenko, G. Dovbeshko, N. Kozlova, S. Suto, A. Watanabe, Thin Solid Films 516 (2008) 8944–8948.
[26] G. Morales, R. van Grieken, A. Martín, F. Martínez, Chem. Eng. J. 161 (2010) 388–396.
[27] B. Gao, D. Kong, Y. Zhang, J. Mol. Catal. A: Chem. 286 (2008) 143–148.
[28] Z.H. Ma, H.B. Han, Z.B. Zhou, J. Nie, J. Mol. Catal. A: Chem. 311 (2009) 46–53.
[29] M.H. Alves, A. Riondel, J.M. Paul, M. Birot, H. Deleuze, C. R. Chimie 13 (2010) 1301–1307.
[30] R.J. Kalbasi, M. Kolahdoozan, A.R. Massah, K. Shahabian, Bull. Korean Chem. Soc. 31 (2010) 2618–2626.
[31] R.J. Kalbasi, M. Kolahdoozan, M. Rezaei, Mater. Chem. Phys. 125 (2011) 784–790.

[32] R.J. Kalbasi, A.A Nourbakhsh, F. Babaknezhad, Catal. Commun. 12 (2011) 955–960.
[33] R.J. Kalbasi, M. Kolahdoozan, K. Shahabian, F. Zamani, Catal. Commun. 11 (2010) 1109–1115.
[34] M.T. Run, S.Z. Wu, D.Y. Zhang, G. Wu, Mater. Chem. Phys. 105 (2007) 341–347.
[35] T. Tsoncheva, L. Ivanova, J. Rosenholm, M. Linden, Appl. Catal. B: Environ. 89 (2009) 365–374.
[36] P. Wang, Z. Wang, J. Li, Y. Bai, Micropor. Mesopor. Mater 116 (2008) 400–405.
[37] T. Iwamoto, K. Matsumoto, T. Matsushita, M. Inokuchi, N Toshima, J. Colloid Interf. Sci. 336 (2009) 879–888.
[38] Ö. Metin, S. Özkar, J. Mol. Catal. A: Chem. 295 (2008) 39–46.
[39] H. Hirai, H. Chawanya, N. Toshima, React. Polym. 3 (1985) 127–141.
[40] H. Song, R.M. Rioux, J.D. Hoefelmeyer, R. Komor, K. Niesz, M. Grass, P. Yang, G.A. Somorjai, J. Am. Chem. Soc. 128 (2006) 3027–3037.
[41] S. Chytil, W.R. Glomm, E. Vollebekk, H. Bergem, J. Walmsley, J. Sjoblom, E.A. Blekkan, Micropor. Mesopor. Mater. 86 (2005) 198–206.
[42] P. Ahmadian Namini, A.A. Babaluo, B. Bayati., Int. J. Nanosci. Nanotechnol. 3 (2007) 37–43.
[43] J. Zhu, Z. Konya, V.F. Puntes, I. Kiricsi, C.X. Miao, J.W. Ager, A.P. Alivisatos, G.A. Somorjai, Langmuir 19 (2003) 4396–4401.
[44] Z. Konya, V.F. Puntes, I. Kiricsi, J. Zhu, A.P. Alivisatos, G.A. Somorjai, Nano Lett. 2 (2002) 907–910.
[45] R.B. Bedford, C.S.J. Cazin, S.J. Coles, T. Gelbrich, P.N. Horton, M.E. Hursthouse, M.E. Light, Organometallics 22 (2003) 987–999.
[46] M. Lamblin, L. Nassar-Hardy, J.-C. Hierso, E. Fouquet, F.-X. Felpin, Adv. Synth. Catal. 352 (2010) 33–79.
[47] P. Anastas, L.G. Heine, T.C. Williamson, Green Chemical Syntheses and Processes, American Chemical Society, Washington DC, 2000.
[48] B. Cornils, W.A. Herrmann, Aqueous-Phase Organometallic Catalysis: Concept and Applications, 2nd and revised Edn., Wiley-VCH, Weinheim, Germany, 2004.
[49] C.-J. Li, Chem. Rev. 105 (2005) 3095–3166.
[50] N. Miyaura, A. Suzuki, Chem. Rev. 95 (1995) 2457–2483.
[51] L. Yin, J. Liebscher, Chem. Rev. 107 (2007) 133–173.
[52] A.F. Littke, G.C. Fu, Angew. Chem. 114 (2002) 4350–4386.
[53] R. Martin, S.L. Buchwald, Acc. Chem. Res. 41 (2008) 1461–1473.
[54] A.F. Littke, C. Dai, G.C. Fu, J. Am. Chem. Soc. 122 (2000) 4020–4028.
[55] H. Weissman, D. Milstein, Chem. Commun. (1999) 1901–1902.
[56] J.P. Wolfe, S.L. Buchwald, Angew. Chem. Int. Ed. 38 (1999) 2413–2416.
[57] X. Cuia, Y. Zhoua, N. Wanga, L. Liu, Q. Guo, Tetrahedron Lett. 48 (2007) 163–167.
[58] N. Marion, O. Navarro, J. Mei, E.D. Stevens, N.M. Scott, S.P. Nolan, J. Am. Chem. Soc. 128 (2006) 4101–4111.
[59] O. Navarro, N. Marion, J. Mei, S.P. Nolan, Chem. Eur. J. 12 (2006) 5142–5148.
[60] I.J.S. Fairlamb, A.R. Kapdi, A.F. Lee, Org. Lett. 6 (2004) 4435–4438.
[61] A. Beeby, S. Bettington, I.J.S. Fairlamb, A.E. Goeta, A.R. Kapdi, E.H. Niemela, A.L. Thompson, New J. Chem. 28 (2004) 600–605.
[62] M. Guo, F. Jian, R. He, Tetrahedron Lett. 47 (2006) 2033–2036.
[63] J.-H. Li, X.-C. Hu, Y.-X. Xie, Tetrahedron Lett. 47 (2006) 9239–9243.
[64] J.-H. Ryu, C.-J. Jang, Y.-S. Yoo, S.-G. Lim, M.J. Lee, Org. Chem. 70 (2005) 8956–8962.
[65] C. Savarin, L.S. Liebeskind, Org. Lett. 3 (2001) 2149–2152.
[66] D. Zim, A.S. Gruber, G. Ebeling, J. Dupont, A.L. Monteiro, Org. Lett. 2 (2000) 2881–2884.
[67] Q. Xu, W.-L. Duan, Z.-Y. Lei, Z.-B. Zhu, M. Shi, Tetrahedron 61 (2005) 11225–11229.
[68] Y. Yu, T. Hu, X. Chen, K. Xu, J. Zhang, J. Huang, Chem. Commun. 47 (2011) 3592–3594.